Determination of the Nucleon-Nucleon Scattering Matrix. X. (p,p) and (n,p) Analysis from 1 to 450 MeV*

MALCOLM H. MACGREGOR, RICHARD A. ARNDT,† AND ROBERT M. WRIGHT
Lawrence Radiation Laboratory, University of California, Livermore, California 94550

(Received 4 November 1968; revised manuscript received 24 February 1969)

Energy-dependent and energy-independent phase-shift analyses are given for (p,p) and (n,p) experiments from 0.5 to 450 MeV. The 2066 data include 1076 (p,p) and 990 (n,p) values. The theoretical analysis has been extended to include magnetic-moment corrections, separate $^1S_0$ phases for (p,p) and (n,p) scattering, S-wave vacuum-polarization effects, and inelastic effects due to pion production with isotopic spin $I=1$ (down to threshold). Precision fits to the data are obtained over the whole energy range. The least-squares sum χ^2 is 1126 for a 26-parameter energy-dependent fit to the (p,p) data. The M value is 1.046. The value for the pion-nucleon coupling constant obtained from this solution is $g^2=14.43\pm0.41$. The $I=1$ scattering matrix is quite accurately and uniquely determined over the whole energy range. Two 26-parameter energy-dependent solutions are given for the fit to the (n,p) data. The first solution (unconstrained) has somewhat anomalous values for ϵ_1 and $^1P_1$ at low energies. The second solution has a constraint that forces ϵ_1 to positive values at low energies. When this is done, the $^1P_1$ phase also changes to values expected from theory. The values of χ^2 (M) from the (n,p) data for these two solutions are 1100 (1.11) and 1138 (1.15), respectively; thus both solutions are statistically acceptable. The (n,p) solution at 425 MeV has been greatly improved by the addition of precise triple-scattering data from the Chicago-Wisconsin group. Comparison of energy-dependent and energy-independent solutions shows that the $I=0$ scattering matrix is fairly accurately determined at 142, 210, and 425 MeV, but at 25, 50, 95, and 330 MeV the solution is not definitive, because of a lack of (n,p) data. Measurement of the ratio $\sigma(180°)/\sigma(90°)$ for (n,p) scattering at 25 or 50 MeV to an accuracy of 1% would help to remove the ambiguity in the ϵ_1 and $^1P_1$ phases. The use of a separate $^1S_0$ phase for (n,p) scattering eliminated the difficulty we formerly had in fitting to (n,p) total cross sections below 100 MeV, and especially at very low energies. The addition of S-wave vacuum-polarization effects permitted a precision fit to the lowest-energy (p,p) differential-cross-section data. The combined (p,p) plus (n,p) 1–450-MeV energy-dependent solution, with 52 parameters representing 27 elastic phases and one inelastic phase, has $\chi^2=2226$ for 2066 data. The M value is 1.077.

I. INTRODUCTION

IN Papers VII–IX in this series,[1–3] we described our phenomenological analysis of the nucleon-nucleon scattering data below 750 MeV. Our principal conclusions were (a) that the isotopic spin 1 ($I=1$) scattering matrix is now well determined up to an energy of 450 MeV, (b) that the $I=1$ scattering matrix cannot be accurately determined at energies above 450 MeV since we have no reliable way of handling large inelastic effects, (c) that the $I=0$ scattering matrix is fairly well determined at energies below 450 MeV, and in particular at energies between 100 and 200 MeV, and (d) that little can be said at the present time about the $I=0$ scattering matrix above 450 MeV.

Since the publication of these papers, there have been several additions to the experimental data, most notably the addition of accurate (n,p) triple-scattering measurements at 425 MeV.[4] There are also several refinements that were not contained in our analyses. These include magnetic-moment corrections, the use of separate $^1S_0$ phases for the (p,p) and (n,p) systems, vacuum polarization corrections to the $^1S_0$ phase, and the addition of small inelastic effects below 400 MeV. With these additions and improvements, we can now define an $I=1$ scattering matrix that is unique, continuous, and statistically well determined over the energy range 1–450 MeV. We can also define an $I=0$ scattering matrix that is continuous and that gives a precision fit to the data over this same energy range. However, the $I=0$ scattering matrix, due to the incompleteness of the data selection, is not everywhere well determined, as is shown by a lack of uniqueness in some of the phases at the lower energies.

In the present paper, we give our reanalysis of (p,p) and (n,p) scattering from 1 to 450 MeV, including the refinements mentioned above, and including a data collection that is complete as of August, 1968. This paper must be read together with Papers VII–IX to obtain a complete description of our analysis. The numerical results given here supersede our previous values. We list the (p,p) energy-dependent solution and two versions of the (n,p) energy-dependent solution. We also list the results of single-energy analyses at 25, 50, 95, 142, 210, 330, and 425 MeV.

At the time the present paper was originally submitted to the Physical Review, one of our principal conclusions was that accurate (n,p) differential cross-section data at low energies would remove the $I=0$

* Work performed under the auspices of the U. S. Atomic Energy Commission.

† Summer visitor at the Lawrence Radiation Laboratory, Livermore, Calif. Present address: Virginia Polytechnic Institute, Blacksburg, Va.

[1] M. H. MacGregor, R. A. Arndt, and R. M. Wright, Phys. Rev. **169**, 1128 (1968).

[2] M. H. MacGregor, R. A. Arndt, and R. M. Wright, Phys. Rev. **169**, 1149 (1968).

[3] M. H. MacGregor, R. A. Arndt, and R. M. Wright, Phys. Rev. **173**, 1272 (1968).

[4] S. C. Wright, D. Shawhan, L. Pondrom, S. Olsen, and R. Handler, Phys. Rev. **175**, 1704 (1968). See Chicago-Wisconsin (1968B) reference in Table II. We would like to thank these authors for supplying us with data prior to publication.

solution ambiguities at those energies. These ambiguities are particularly evident in the ϵ_1 and $^1P_1$ phases. We have subsequently received new (n,p) differential cross-section data at 24 MeV from Wisconsin. Since these data have an appreciable effect on the solution, we have incorporated them into the analysis and have revised the present paper so as to present the latest results.

II. REFINEMENTS IN THE ANALYSIS

Vacuum polarization was handled in our previous analysis[1] by applying corrections to the $l \geq 1$ phases.[5] However, we did not apply the important correction to the $^1S_0$ phase. Thus our solution was not accurate at energies below 2 MeV. We have now included the vacuum-polarization correction to the (p,p) $^1S_0$ phase.[6] With this addition, we obtain a precision fit to the Wisconsin differential-cross-section data at 1.397 MeV.[5]

Magnetic-moment corrections have been derived by Breit and co-workers,[7] and have been applied to the Yale[8] and Harwell analyses.[9] Perring[9] applied the magnetic-moment correction to F waves and higher in his (p,p) analysis. Thus his phase shifts are pure nuclear for F waves and are nuclear plus magnetic moment for P waves (the magnetic-moment correction only operates on triplet spin states in the $I=1$ system). Since there is at present no reliable way in which nuclear and magnetic-moment effects can be separated for P-waves, we decided to avoid this mixed representation for the phases by applying magnetic-moment corrections only to the higher phases calculated from one pion exchange (OPE). When applied in this manner to $I=1$ phases, the magnetic-moment correction is a very small one (and is in fact comparable to uncertainties present in any handling of the OPE calculation). The Livermore $I=1$ analysis thus includes low-l phenomenological phases that are a combination of nuclear plus magnetic-moment effects, together with high-l phases that are a sum of OPE and magnetic-moment contributions.

Magnetic-moment corrections were not applied to the $I=0$ phases. The $I=0$ uncertainties are so large at present that they completely mask any possible magnetic-moment effects. Also, the (n,p) magnetic-moment correction includes an isotopic-spin-violating component that we cannot handle in our present computational formalism. Thus we have no consistent way of including $I=0$ magnetic-moment effects. They are in any case very small when applied only to OPE phases.

The most recent Yale phase-shift analysis[8] included the use of separate $^1S_0$ phases for the (p,p) and (n,p) systems. The phases were not searched independently, but rather were kept at a constant difference that was precalculated at each energy from a potential model. In our recent analysis of the (n,p) system,[3] we did not use a splitting for the $^1S_0$ phase. We showed in our single-energy analyses that the data at present do not strongly point to any splitting for the $^1S_0$ phase. However, we experienced a difficulty[3] in fitting to (n,p) total cross sections at low energies (especially below 4 MeV, but even up to 100 MeV) that was attributable to our failure to introduce a charge dependence for the $^1S_0$ phase. In the present work, we carry out energy-dependent analyses by using separate $^1S_0$ phases for the (p,p) and the (n,p) systems. The (p,p) S phase has as its asymptotic lower limit the effective-range expansion appropriate for (p,p) scattering[10] ($a=-7.815$ F, $r=2.795$ F). (It also has the Heller vacuum-polarization corrections.[6]) The (n,p) $^1S_0$ phase has as its asymptotic lower limit the effective-range expansion appropriate for (n,p) scattering[11] ($a=-23.679$ F, $r=2.51$ F). The (n,p) $^3S_1$ phase has as its asymptotic lower limit the corresponding values[11] ($a=5.397$ F, $r=1.727$ F). When we introduced this form for the analysis, our difficulty in fitting to (n,p) total cross sections vanished. We now obtain a precision fit at very low energies (0.49 MeV), and the solution, somewhat to our surprise, gives a good statistical fit to all of the (n,p) total cross-section data below 100 MeV (see a discussion of this point in Sec. II of Paper IX).

Our single-energy analyses in the present paper were initially carried out using separate (p,p) and (n,p) $^1S_0$ phases. However, at 210 MeV this leads to rather large uncertainties in the (n,p) $^1S_0$ phase, and at 330 and 425 MeV it leads to ambiguous $I=0$ phases. Thus at 330 and 425 MeV, where the $^1S_0$ splitting is probably rather small,[8] we removed the splitting in $^1S_0$ for the single-energy solutions.

We also investigated the effect of using separate (p,p) and (n,p) phases for $^1D_2$ and $^3P_0$, as described in Sec. III. However, as expected, it appears that this extra charge-dependent freedom is not warranted at the present time.

[5] D. J. Knecht, P. F. Dahl, and S. Messelet, Phys. Rev. **148**, 1031 (1966), and references therein.

[6] L. Heller, Phys. Rev. **120**, 627 (1960).

[7] G. Breit and R. D. Haracz, in *High Energy Physics*, edited by E. H. S. Burhop (Academic Press Inc., New York, 1967), Vol. I, p. 21; G. Breit and H. M. Ruppel, Phys. Rev. **127**, 2123 (1962); **131**, 2839 (1963).

[8] R. E. Seamon, K. A. Friedman, G. Breit, R. D. Haracz, J. M. Holt, and A. Prakash, Phys. Rev. **165**, 1579 (1968).

[9] The latest results of Perring are quoted in the Harwell 1968A reference of Table II. Note that the relatively poor fit shown for the Livermore solution to the 97.7-MeV polarization data in Fig. 6 of this reference is due to the fact that the Harwell authors inadvertently used the Livermore phase shifts, which were uncorrected for magnetic-moment effects, in an observable code set up by Perring which includes magnetic-moment corrections to F waves and higher. When this discrepancy in the observable calculation is removed, the Livermore curve falls between the Perring and Yale curves in Fig. 6 (private communication from O. N. Jarvis). This example is instructive in showing the magnitude of the magnetic-moment effects as applied to F waves and higher.

[10] H. P. Noyes, Phys. Rev. Letters **12**, 171 (1964); see Eq. (6) in Ref. 1.

[11] H. P. Noyes, Phys. Rev. **130**, 2025 (1963).

TABLE I. New (p,p) and (n,p) data from 0.5 to 450 MeV. Only data that are not as described in Table I of Papers VII–IX are included.

Energy (MeV)	No., type data	Angular range (c.m.) (deg)	Data std. err. (%)	Norm. std. err. (%)	Deleted angles	Comment	Ref.
			(p,p) data				
6.141	17σ	12–100	0.5	0.1[a]		b, c	Berkeley (1968)
6.141	17σ	12–100	0.5	0.1[a]		b, d	Berkeley (1968)
8.097	16σ	12–90	0.5	0.1[a]		b, c	Berkeley (1968)
8.097	16σ	12–90	0.5	0.1[a]		b, d	Berkeley (1968)
9.918	17σ	12–100	0.5	0.1[a]		b, c	Berkeley (1968)
9.918	17σ	12–100	0.5	0.1[a]		b, d	Berkeley (1968)
20.2	$8P$	35–90	100	11.8			Saclay (1968)
52.34	25σ	14–90	0.5	0.53	16°, 18°, 20°	e	Tokyo (1968)
97.7	$13P$	16–89	3	0.85		f	Harwell (1968A)
98.8	19σ	22–89	1	1.0			Harwell (1968A)
140.7	$20P$	17–112	2	0.85		g	Harwell (1968B)
144.1	6σ	16–36	0.7	0.88		e	Harwell (1968B)
144.1	15σ	41–112	0.5	0.56		e	Harwell (1968B)
305.0	$14C_{NN}$	60–104	15	8.0		h	Chicago (1968)
330.0	$13C_{NN}$	60–100	20	8.0		h	Chicago (1968)
330.0	$1\sigma_R$		67			i	CERN (1968)
358.0	$14C_{NN}$					j	Chicago (1968)
370.0	$1\sigma_R$		25			k	CERN (1968)
386.0	$14C_{NN}$	58–101	15	8.0		h	Chicago (1968)
400.0	$1\sigma_R$		15			l	CERN (1968)
415.0	$14P$	52–97	10	4.7			Chicago (1968)
415.0	$14C_{NN}$	52–97	10	8.0		h	Chicago (1968)
430.0	$1P$	65	5				Chicago-Wisconsin (1968A)
430.0	$2D$, $2R$, $2A$, $2R'$, $2A'$					m	Chicago-Wisconsin (1968A)
			(n,p) data				
0.4926	$1\sigma_T$		0.2			n	Columbia (1963)
1.005	$1\sigma_T$		0.5			n	Wisconsin (1954)
1.312	$1\sigma_T$		0.5			n	M.I.T. (1954)
2.530	$1\sigma_T$		0.4			n	Wisconson (1954)
3.186	$1\sigma_T$		0.4			n	Columbia (1963)
4.748	$1\sigma_T$		0.4			n	Brookhaven (1952)
14.1	4σ		1				Kyoto (1960)
15.8–96.0	$22\sigma_T$					o	Harwell (1961)
24.0	4σ		~1.5				Wisconsin (1969)
350.0	$10P$				85°, 126°	p	Carnegie (1956)
425.0	$3P$	44, 65, 90	10	4.7		q	Chicago-Wisconsin (1968B)
425.0	$3D$	44, 65, 90	5			q	Chicago-Wisconsin (1968B)
425.0	$3R$	44, 65, 90	8			q	Chicago-Wisconsin (1968B)
425.0	$3A$	44, 65, 90	8			q	Chicago-Wisconsin (1968B)

[a] This small normalization uncertainty was added by the present authors.
[b] Vacuum-polarization corrections for $l \geq 1$ were kindly supplied by R. J. Slobodrian and were applied to these data.
[c] Data set BGS. This set was selected in preference to data set D, since it was more compatible with neighboring measurements. However, the shape of the differential cross section at 9.918 MeV seems to differ systematically from the shapes at neighboring energies.
[d] Data set D. This set was deleted in favor of set BGS.
[e] These data are in final form.
[f] These data replace the data formerly listed at 93.2 MeV.
[g] These data replace the data formerly listed at 140 MeV.
[h] These are final data and differ from the preliminary data used earlier mainly in the over-all normalization assignment. We would like to thank N. E. Booth for supplying us with these data.
[i] The total reaction cross-section value 0.3 ± 0.2 mb was used here.
[j] These data were deleted by the experimenters.
[k] The total reaction cross-section value 0.8 ± 0.2 mb was used here.
[l] The total reaction cross-section value 1.4 ± 0.2 mb was used here.
[m] These are the values that were listed at 425 MeV in Table I of Paper VIII.
[n] These data are from J. C. Davis and H. H. Barschall, Phys. Letters (to be published).
[o] These data were excluded from our previous analysis because of space limitations in the computer code. They have been included in the present analysis as 22 individual points. Our analysis now gives a statistically acceptable fit to all of the (n,p) total cross-section data below 100 MeV, as shown in Table V.
[p] The individual points deleted are more than three standard deviations away from the theoretical curve.
[q] These data are from a polarized proton beam incident on the deuterium target. No corrections were applied for deuteron binding effects.

Inelastic effects were ignored in Paper VII, which was an analysis below 400 MeV. They were included in Paper VIII for energies above 400 MeV. In the present paper, we have included inelastic effects in the $I=1$ amplitudes by introducing five values of the total reaction cross section[12] between 330 and 450 MeV. The inelasticity was attributed to the $^1D_2$ phase, and an energy-dependent form was used with a threshold at 280 MeV, with a suitable behavior near threshold, and with a single adjustable parameter of the form described in Sec. III of Paper VIII. No inelasticity was included for the $I=0$ amplitudes, which cannot couple to the (3,3) resonance. This is in agreement with the results of the Measday compilation.[12]

[12] See CERN (1968) reference in Table II.

III. CHANGES IN THE (p,p) AND (n,p) DATA

Tables I and II in Papers VII–IX gave our listing of the (p,p) and (n,p) data from 1 to 750 MeV. Tables I and II of the present paper give the changes and

TABLE II. References for Table I.

		(p,p) data
Berkeley	(1968)	R. J. Slobodrian, H. E. Conzett, E. Schield and W. F. Tivol, Phys. Rev. **174**, 1122 (1968).
CERN	(1968)	These values are from a graph supplied to us by D. Measday and are taken from a review article he is writing while at CERN.
Chicago	(1968)	A. Beretvas, Phys. Rev. **171**, 1392 (1968).
Harwell	(1968A)	M. R. Wigan, R. A. Bell, P. J. Martin, O. N. Jarvis, and J. P. Scanlon, Nucl. Phys. **A114**, 377 (1968).
Harwell	(1968B)	G. F. Cox, G. H. Eaton, C. P. van Zyl, O. N. Jarvis, and B. Rose, Nucl. Phys. **B4**, 353 (1968).
Saclay	(1968)	P. Catillon, J. Sura, and A. Tarrats, Phys. Rev. Letters **20**, 602 (1968).
Tokyo	(1968)	This is the last reference listed under Tokyo (1967) in Table II of Paper VII.
Chicago-Wisconsin	(1968A)	P. Limon, L. Pondrom, S. Olsen, P. Kloeppel, R. Handler, and S. C. Wright, Phys. Rev. **169**, 1026 (1968).
		(n,p) data
Brookhaven	(1952)	The original data are by E. M. Hafner, W. F. Hornyak, C. E. Falk, G. Snow, and T. Coor, Phys. Rev. **89**, 204 (1952), and are used as noted in footnote n to Table I.
Carnegie	(1956)	R. T. Siegel, A. J. Hartzler, and W. A. Love, Phys. Rev. **101**, 838 (1956).
Chicago-Wisconsin	(1968B)	S. C. Wright, D. Shawhan, L. Pondrom, S. Olsen, and R. Handler, Phys. Rev. **175**, 1704 (1968).
Columbia	(1963)	The original data are by C. E. Engelke, R. E. Benenson, E. Melkonian, and J. M. Lebowitz, Phys. Rev. **129**, 324 (1963), and are used as noted in footnote n to Table I.
Harwell	(1961)	P. H. Bowen, J. P. Scanlon, G. H. Stafford, J. J. Thresher, and P. E. Hodgson, Nucl. Phys. **22**, 640 (1961).
Kyoto	(1960)	See Ref. 15.
Wisconsin	(1969)	See Ref. 16.
M.I.T.	(1954)	The original data are by C. L. Storrs and D. H. Frisch, Phys. Rev. **95**, 1252 (1954), and are used as noted in footnote n to Table I.
Wisconsin	(1954)	The original data are by R. E. Fields, R. L. Becker, and R. K. Adair, Phys. Rev. **94**, 389 (1954), and are used as noted in footnote n to Table I.

additions to the data between 1 and 450 MeV that have been applied in the present analysis.

Most of the data shown in Table I are slightly updated versions of data that we have already included in our previous analyses.[1–3] However, the Berkeley (p,p) differential cross-section data at 6.141, 8.097, and 9.918 MeV, the Saclay (p,p) polarization data at 20.2 MeV, the Harwell (p,p) differential-cross-section data at 98.8 MeV, and the Chicago-Wisconsin (n,p) triple-scattering data at 425 MeV are new. The references for Table I are listed in Table II.

The only new data that led to real difficulties were the Berkeley (p,p) differential-cross-section data.[13] As we have discussed in another publication,[14] our phase-shift solution shows a preference for the BGS data over the D data (these are two different ways of subtracting background effects). In addition, the BGS data at 9.918 MeV [13] seem to be incompatible in shape with the nearby (p,p) data of our compilation, and also with the BGS data at 6.141 and 8.097 MeV measured in the same experiment.[13] Nevertheless, we have retained the 9.918-MeV BGS data in our compilation, since their effect on the energy-dependent solution is slight.

The new (n,p) data at 425 MeV [4] represent a decisive improvement, since our previous (n,p) data compilation[3] below 450 MeV had no useful (n,p) triple-scattering data above 212 MeV. The new measurements[4] include (n,p) P, D, R, and A measurements at each of three angles, with quoted statistical uncertainties of 10% or less. A polarized proton beam was used for the measurements. No corrections were made for binding in the deuterium target, but at these energies and angles the correction hopefully is not large.

The Kyoto 14.1-MeV (n,p) differential cross-section data[15] listed in Table I show a marked 180°/90° asymmetry. The fit to these data for the solutions of November, 1968, is very poor (an M value of about 6). These data were not included in our original analysis. However, the new Wisconsin (n,p) differential-cross-section data at 24 MeV [16] also show a marked 180°/90° asymmetry. These two experiments are somewhat at variance with other (n,p) data in this energy range. Since we have no way of selecting among these data, we have added both the Kyoto and Wisconsin data to the (n,p) compilation. On theoretical grounds, there is some reason to expect an appreciable 180°/90° asymmetry at these energies.[17] This subject is discussed in detail in Sec. V.

[13] See BERKELEY (1968) reference in Table II.

[14] M. H. MacGregor, R. A. Arndt, and R. M. Wright, Phys. Rev. **179**, 1624 (1969).

[15] Kyoto (1960): T. Nakamura, J. Phys. Soc. Japan **15**, 1359 (1960). J. Hopkins called this reference to our attention.

[16] Wisconsin (1969): L. N. Rothenberg and T. G. Masterson, Bull. Am. Phys. Soc. **14**, 511 (1969); L. N. Rothenberg (private communication). The data we used, which should be regarded as preliminary, are the following: 89°, 30.3±0.46 mb; 118°, 31±0.57 mb; 146°, 32.8±0.51 mb; 165°, 34.4±0.43 mb.

[17] See Ref. 7, Chap. 2, first reference of footnote 15, pp. 127–128; see also D. Y. Wong, Phys. Rev. Letters **2**, 406 (1959).

TABLE III. (p,p) data from 1.4 to 450 MeV. The data used in the final analyses are listed together with the M values (χ^2 average per data point) and the normalization constant obtained from the 26-parameter analysis. $g^2=14.43$ for the OPE phases. $\chi^2=1126$ for 1076 data, so the over-all M value is 1.046.

Energy (MeV)	Data	M value	Predicted norm.[a]	Energy (MeV)	Data	M value	Predicted norm.[a]	Energy (MeV)	Data	M value	Predicted norm.[a]	Energy (MeV)	Data	M value	Predicted norm.[a]
1.397	1σ	0.9	0.999	51.5	1σ	0.9		137.0	3σ	0.1	0.981	320.0	$1C_{NN}$	1.3	
1.855	13σ	1.3	0.998	51.5	9σ	0.9	0.940	137.0	$3P$	1.0	0.979	328.0	$13P$	0.6	0.948
2.425	14σ	0.2	0.999	51.7	$1P$	0.5		137.5	$5R'$	0.1		330.0	16σ	1.4	0.892
3.037	13σ	0.9	0.998	51.8	9σ	1.7	0.949	138.0	$4D$	1.3		330.0	$13C_{NN}$	0.4	0.937
6.141	17σ	1.7	1.002	52.0	$1C_{NN}$	2.2		139.0	$6A$	0.6	0.964	330.0	$1\sigma_R$	0.3	
8.097	16σ	1.3	1.001	52.0	$1C_{KP}$	3.0		140.0	$6R$	1.0		345.0	10σ	1.4	0.883
9.68	1σ	1.3		52.34	26σ	0.8	0.998	140.4	$6R'$	1.2		345.0	17σ	1.8	1.005
9.69	26σ	0.8	1.016	53.2	$1P$	1.8		140.7	$20P$	1.0	1.007	370.0	$1\sigma_R$	1.1	
9.918	17σ	2.4	1.000	56.0	$1P$	0.1		142.0	$27P$	1.3	1.049	380.0	10σ	1.3	1.029
11.4	$1C_{NN}$	0.3		56.15	1σ	0.1		142.0	$8R$	1.0		380.0	6σ	0.6	1.005
11.4	$1A_{XX}$	0.0		58.5	$1P$	0.7		142.0	$8D$	1.7		382.0	$1C_{NN}$	2.2	
14.16	17σ	0.1	0.992	61.92	1σ	0.1		143.0	$7D$	0.5		382.0	$1C_{KP}$	1.4	
16.2	$1P$	0.7		66.0	10σ	0.1	1.041	143.0	$6A$	0.9		386.0	$14C_{NN}$	1.7	0.826
18.2	8σ	0.7	1.002	66.0	$11P$	1.0	1.030	143.0	$2C_{NN}$	0.1		400.0	$2C_{NN}$	0.5	
19.2	$1C_{NN}$	0.0		68.3	26σ	1.3	1.014	144.1	6σ	0.6	1.004	400.0	$2C_{KP}$	1.7	
19.2	$1A_{XX}$	0.1		68.42	1σ	0.3		144.1	15σ	0.9	1.002	400.0	$7P$	0.8	1.038
20.2	$8P$	0.2	0.979	69.5	1σ	0.0		147.0	$28P$	1.1	1.009	400.0	$7P$	1.4	1.006
23.5	$1C_{NN}$	0.1		70.0	$1P$	2.6		155.0	23σ	1.4	0.975	400.0	$1\sigma_R$	1.8	
23.5	$1A_{XX}$	0.4		71.0	$1P$	0.6		170.0	$7P$	0.4	0.980	415.0	$14P$	0.8	0.986
25.63	23σ	0.5	1.099	73.5	$1C_{NN}$	0.5		174.0	$5P$	0.9	0.937	415.0	$7P$	0.5	0.969
26.5	$1C_{NN}$	0.6		78.0	$1P$	0.6		210.0	$6P$	0.5	0.976	415.0	$1D$	2.4	
26.5	$1A_{XX}$	2.6		78.5	1σ	0.0		210.0	7σ	1.9	0.966	415.0	$14C_{NN}$	1.3	0.811
27.0	$1C_{NN}$	0.2		86.0	$1P$	0.0		213.0	13σ	1.7	0.990	419.0	7σ	2.0	0.844
27.6	$3A$	1.5	0.996	95.0	6σ	0.1	0.997	213.0	$13P$	1.1	0.993	430.0	$1P$	1.1	
27.6	$2R$	0.5	0.992	95.0	6σ	0.4	1.019	213.0	$7R$	0.2		430.0	$2D$	0.2	
28.16	1σ	1.3		95.0	1σ	0.1		213.0	$5R'$	2.1		430.0	$2R$	1.4	
30.0	$1P$	4.5		95.0	13σ	0.2	0.979	213.0	$7D$	0.6		430.0	$2A$	2.0	
31.15	1σ	0.2		95.0	$14P$	1.3	0.995	213.0	$5E$	0.8		430.0	$2R'$	1.0	
34.2	1σ	0.4		97.0	$1P$	3.0		213.0	$2A$	0.8		430.0	$2A'$	0.4	
36.9	1σ	0.0		97.7	$13P$	0.9	0.994	276.0	$6P$	1.7	0.875	430.0	$6P$	1.2	0.968
39.4	27σ	1.1	0.987	98.0	$14P$	1.1	0.979	305.0	$14C_{NN}$	1.2	0.882	430.0	$7D$	0.5	
39.6	1σ	0.1		98.0	$1C_{NN}$	0.0		310.0	7σ	1.5	1.039	430.0	$7R$	0.8	
41.0	1σ	0.8		98.0	$5R$	1.3		310.0	$7P$	0.6	0.991	430.0	$7A$	1.8	
44.66	1σ	1.3		98.0	$4R'$	0.2		310.0	$6P$	1.4	0.951	430.0	$7A'$	3.0	
46.0	$1P$	1.5		98.0	$5D$	1.1		310.0	$6R$	1.7		431.0	$1\sigma_R$	0.3	
47.5	$5A$	1.7	0.980	98.8	19σ	1.5	1.008	310.0	$6D$	0.9		437.0	8σ	0.3	0.958
47.8	$5A$	0.4	1.019	102.0	3σ	2.0	0.991	315.0	7σ	1.2	0.967	450.0	$1C_{NN}$	2.0	
47.8	$5R$	1.0	0.999	102.0	$3P$	0.8	1.025	315.0	$6P$	1.2	0.922	450.0	$1C_{KP}$	0.2	
49.4	28σ	1.2	0.998	107.0	3σ	0.1	0.935	315.0	$1C_{NN}$	0.5		450.0	$1\sigma_R$	1.8	
49.9	$1P$	0.1		118.0	15σ	1.4	0.956	315.0	$1C_{NN}$	0.0					
50.0	$1D$	1.2		127.0	3σ	0.0	0.957	315.0	$1C_{KP}$	0.0					
50.17	1σ	0.4		130.0	$4P$	0.7	0.983	316.0	$3A$	1.3					

[a] This is the theoretical normalization constant. The renormalization of the experimental data is the reciprocal of this quantity.

IV. (p,p) ENERGY-DEPENDENT ANALYSES

These analyses are similar to the analyses described in Papers VII and VIII, except that now we use the data revisions listed in Table I, we include magnetic-moment and vacuum-polarization corrections, we allow for the correct total inelasticity (atrributed to the $^1D_2$ phase) down to threshold, and we cover the energy range 1.397–450 MeV.

In Paper VII, we quoted a 23-parameter solution as being the most useful (see Table IV of that paper). In the present work we made an extensive reexamination of the required number of free parameters. With the new data set (1076 data), we obtained a least-squares sum $\chi^2=1184$ with the former choice of 23 elastic parameters, plus one inelastic parameter for the $^1D_2$ phase. It was found that by adding one more free parameter each to the $^1D_2$ and $^3F_3$ phases, we could reduce χ^2 to 1126. By adding an additional five parameters, we could further reduce χ^2 to a minimum value of 1113. However, the most useful solution in our opinion is the solution containing 25 phenomenological elastic parameters plus one phenomenological inelastic parameter, and we quote this 26-parameter representation as our final solution.

The data used for the (p,p) analysis, including the χ^2 per data point average (the M value) and the theoretical normalization constants obtained in the matrix search, are listed in Table III. Since there are 1076 data and the χ^2 sum is 1126, the M value for the energy-dependent solution is 1.046. Statistically speaking, this fit to the data is quantitatively about as good as one would ever hope to achieve. The energy range spanned by the solution is 1.397–450 MeV, and the total number of adjustable phase shift parameters required is 26. The fact that the Yale group, using a completely different parametrization than ours, have

TABLE IV. (p,p) phase shifts for the 26-parameter energy-dependent solution. The χ^2 value for this solution is 1126, and the 1076 data are described in Table III. $g^2=14.43$.

Energy (MeV)	$^1S_0$	$^1D_2$	$^1G_4$	$^3P_0$	$^3P_1$
1	32.69±0.00	0.00±0.00	0.00±0.00	0.20±0.00	−0.13±0.00
2	45.58±0.01	0.01±0.00	0.00±0.00	0.53±0.00	−0.33±0.00
3	50.90±0.01	0.02±0.00	0.00±0.00	0.91±0.01	−0.56±0.00
4	53.42±0.01	0.03±0.00	0.00±0.00	1.32±0.01	−0.80±0.00
5	54.68±0.02	0.05±0.00	0.00±0.00	1.74±0.02	−1.05±0.01
6	55.27±0.02	0.07±0.00	0.00±0.00	2.16±0.02	−1.30±0.01
8	55.48±0.03	0.12±0.00	0.00±0.00	2.98±0.03	−1.79±0.01
10	55.08±0.04	0.18±0.00	0.00±0.00	3.77±0.04	−2.26±0.01
12	54.41±0.04	0.25±0.00	0.01±0.00	4.52±0.05	−2.70±0.02
14	53.61±0.05	0.32±0.00	0.01±0.00	5.22±0.06	−3.12±0.02
16	52.76±0.05	0.39±0.00	0.02±0.00	5.86±0.07	−3.52±0.02
18	51.88±0.06	0.46±0.00	0.02±0.00	6.46±0.08	−3.89±0.02
20	51.00±0.06	0.53±0.01	0.03±0.00	7.02±0.09	−4.25±0.03
25	48.81±0.07	0.72±0.01	0.04±0.00	8.21±0.11	−5.08±0.03
30	46.70±0.07	0.92±0.01	0.06±0.00	9.18±0.13	−5.82±0.04
40	42.75±0.09	1.31±0.01	0.11±0.00	10.52±0.16	−7.14±0.05
50	39.14±0.10	1.72±0.02	0.17±0.00	11.26±0.19	−8.31±0.06
60	35.84±0.12	2.12±0.02	0.22±0.00	11.55±0.21	−9.38±0.06
70	32.81±0.13	2.53±0.03	0.28±0.00	11.52±0.22	−10.39±0.06
80	30.02±0.15	2.93±0.04	0.33±0.00	11.22±0.23	−11.35±0.06
90	27.44±0.16	3.33±0.04	0.38±0.01	10.74±0.23	−12.29±0.06
100	25.04±0.17	3.73±0.05	0.44±0.01	10.11±0.24	−13.19±0.06
120	20.69±0.20	4.49±0.06	0.54±0.01	8.53±0.24	−14.94±0.06
140	16.84±0.22	5.22±0.07	0.64±0.02	6.68±0.23	−16.64±0.07
160	13.34±0.25	5.90±0.08	0.73±0.02	4.69±0.23	−18.28±0.08
180	10.13±0.27	6.52±0.09	0.82±0.03	2.63±0.24	−19.88±0.09
200	7.12±0.28	7.10±0.10	0.91±0.04	0.56±0.25	−21.43±0.11
220	4.27±0.30	7.63±0.11	0.99±0.04	−1.50±0.27	−22.94±0.13
240	1.55±0.32	8.11±0.12	1.07±0.05	−3.51±0.30	−24.42±0.15
260	−1.09±0.33	8.54±0.13	1.15±0.06	−5.47±0.33	−25.85±0.17
280	−3.64±0.35	8.93±0.14	1.22±0.07	−7.37±0.37	−27.25±0.19
300	−6.14±0.38	9.27±0.16	1.30±0.08	−9.19±0.41	−28.61±0.21
320	−8.60±0.42	9.58±0.18	1.37±0.08	−10.94±0.46	−29.93±0.23
340	−11.01±0.47	9.85±0.20	1.43±0.09	−12.62±0.50	−31.22±0.25
360	−13.39±0.54	10.08±0.22	1.50±0.10	−14.22±0.54	−32.47±0.27
380	−15.75±0.61	10.28±0.25	1.56±0.11	−15.75±0.59	−33.69±0.29
400	−18.07±0.70	10.46±0.27	1.63±0.12	−17.21±0.63	−34.88±0.31
420	−20.38±0.80	10.60±0.30	1.69±0.13	−18.59±0.68	−36.04±0.33
440	−22.67±0.90	10.72±0.33	1.75±0.14	−19.91±0.72	−37.17±0.35
460	−24.93±0.12	10.81±0.37	1.80±0.14	−21.16±0.76	−38.27±0.37

Energy (MeV)	$^3P_2$	ϵ_2	$^3F_2$	$^3F_3$	$^3F_4$
1	0.02±0.00	−0.00±0.00	0.00±0.00	−0.00±0.00	0.00±0.00
2	0.06±0.00	−0.01±0.00	0.00±0.00	−0.00±0.00	0.00±0.00
3	0.12±0.00	−0.02±0.00	0.00±0.00	−0.00±0.00	0.00±0.00
4	0.18±0.01	−0.04±0.00	0.00±0.00	−0.00±0.00	0.00±0.00
5	0.26±0.01	−0.06±0.00	0.00±0.00	−0.01±0.00	0.00±0.00
6	0.34±0.01	−0.09±0.00	0.00±0.00	−0.01±0.00	0.00±0.00
8	0.53±0.01	−0.15±0.00	0.01±0.00	−0.02±0.00	0.00±0.00
10	0.73±0.02	−0.22±0.00	0.01±0.00	−0.04±0.00	0.00±0.00
12	0.95±0.02	−0.30±0.00	0.02±0.00	−0.06±0.00	0.00±0.00
14	1.18±0.02	−0.38±0.00	0.03±0.00	−0.08±0.00	0.00±0.00
16	1.43±0.03	−0.47±0.00	0.04±0.00	−0.10±0.00	0.01±0.00
18	1.68±0.03	−0.55±0.00	0.05±0.00	−0.13±0.00	0.01±0.00
20	1.93±0.03	−0.64±0.01	0.07±0.00	−0.16±0.00	0.01±0.00
25	2.59±0.04	−0.85±0.01	0.10±0.00	−0.24±0.00	0.02±0.00
30	3.26±0.04	−1.05±0.01	0.14±0.00	−0.33±0.00	0.04±0.00
40	4.58±0.05	−1.41±0.02	0.22±0.00	−0.51±0.01	0.08±0.00
50	5.86±0.05	−1.73±0.02	0.29±0.01	−0.69±0.01	0.12±0.00
60	7.05±0.04	−1.99±0.03	0.37±0.01	−0.87±0.02	0.18±0.00
70	8.17±0.04	−2.22±0.03	0.43±0.01	−1.03±0.03	0.25±0.01
80	9.19±0.04	−2.39±0.03	0.49±0.02	−1.18±0.03	0.32±0.01
90	10.13±0.04	−2.54±0.04	0.54±0.02	−1.32±0.04	0.40±0.01
100	10.99±0.05	−2.66±0.04	0.58±0.03	−1.45±0.05	0.48±0.01
120	12.48±0.05	−2.82±0.04	0.65±0.04	−1.69±0.06	0.65±0.02
140	13.70±0.06	−2.90±0.04	0.69±0.05	−1.91±0.07	0.83±0.02
160	14.68±0.06	−2.92±0.05	0.71±0.07	−2.10±0.08	1.02±0.03
180	15.47±0.07	−2.89±0.05	0.71±0.08	−2.28±0.09	1.21±0.04
200	16.09±0.08	−2.82±0.06	0.71±0.10	−2.44±0.10	1.40±0.04
220	16.57±0.08	−2.72±0.07	0.69±0.11	−2.60±0.10	1.59±0.05

TABLE IV. (*continued*).

Energy (MeV)	$^3P_2$	ϵ_2	$^3F_2$	$^3F_3$	$^3F_4$
240	16.92±0.09	−2.60±0.08	0.66±0.13	−2.75±0.11	1.78±0.06
260	17.17±0.11	−2.45±0.10	0.62±0.14	−2.90±0.11	1.97±0.06
280	17.33±0.12	−2.30±0.12	0.58±0.16	−3.04±0.12	2.16±0.07
300	17.41±0.14	−2.13±0.14	0.54±0.17	−3.18±0.12	2.35±0.08
320	17.42±0.17	−1.95±0.16	0.49±0.19	−3.31±0.13	2.53±0.08
340	17.38±0.19	−1.76±0.18	0.44±0.20	−3.44±0.14	2.70±0.09
360	17.29±0.22	−1.57±0.20	0.39±0.21	−3.57±0.15	2.88±0.10
380	17.15±0.25	−1.37±0.23	0.33±0.23	−3.70±0.16	3.05±0.10
400	16.98±0.28	−1.17±0.25	0.28±0.24	−3.83±0.18	3.22±0.11
420	16.78±0.31	−0.97±0.27	0.22±0.26	−3.96±0.19	3.38±0.12
440	16.55±0.34	−0.77±0.29	0.17±0.27	−4.09±0.21	3.54±0.12
460	16.29±0.37	−0.57±0.32	0.11±0.28	−4.21±0.23	3.70±0.13

Energy (MeV)	ϵ_4	$^3H_4$	$^3H_5$	$^3H_6$
1	−0.00±0.00	0.00±0.00	−0.00±0.00	0.00±0.00
2	−0.00±0.00	0.00±0.00	−0.00±0.00	0.00±0.00
3	−0.00±0.00	0.00±0.00	−0.00±0.00	0.00±0.00
4	−0.00±0.00	0.00±0.00	−0.00±0.00	0.00±0.00
5	−0.00±0.00	0.00±0.00	−0.00±0.00	0.00±0.00
6	−0.00±0.00	0.00±0.00	−0.00±0.00	0.00±0.00
8	−0.00±0.00	0.00±0.00	−0.00±0.00	0.00±0.00
10	−0.00±0.00	0.00±0.00	−0.00±0.00	0.00±0.00
12	−0.01±0.00	0.00±0.00	−0.00±0.00	0.00±0.00
14	−0.01±0.00	0.00±0.00	−0.00±0.00	0.00±0.00
16	−0.02±0.00	0.00±0.00	−0.00±0.00	0.00±0.00
18	−0.02±0.00	0.00±0.00	−0.01±0.00	0.00±0.00
20	−0.03±0.00	0.00±0.00	−0.01±0.00	0.00±0.00
25	−0.05±0.00	0.00±0.00	−0.02±0.00	0.00±0.00
30	−0.08±0.00	0.01±0.00	−0.03±0.00	0.00±0.00
40	−0.14±0.00	0.02±0.00	−0.06±0.00	0.00±0.00
50	−0.20±0.00	0.03±0.00	−0.09±0.00	0.01±0.00
60	−0.27±0.00	0.04±0.00	−0.13±0.00	0.01±0.00
70	−0.34±0.00	0.05±0.00	−0.18±0.00	0.02±0.00
80	−0.41±0.00	0.07±0.00	−0.23±0.00	0.02±0.00
90	−0.48±0.01	0.08±0.00	−0.28±0.01	0.03±0.00
100	−0.54±0.01	0.10±0.01	−0.33±0.01	0.04±0.00
120	−0.66±0.01	0.13±0.01	−0.43±0.01	0.06±0.01
140	−0.76±0.02	0.15±0.02	−0.53±0.02	0.08±0.01
160	−0.86±0.03	0.18±0.02	−0.63±0.03	0.10±0.01
180	−0.94±0.03	0.20±0.03	−0.73±0.04	0.12±0.02
200	−1.01±0.04	0.22±0.04	−0.82±0.05	0.15±0.02
220	−1.08±0.05	0.23±0.05	−0.90±0.06	0.17±0.03
240	−1.14±0.06	0.24±0.06	−0.99±0.08	0.20±0.04
260	−1.19±0.07	0.25±0.07	−1.07±0.09	0.22±0.04
280	−1.24±0.08	0.26±0.09	−1.14±0.11	0.25±0.05
300	−1.28±0.09	0.26±0.10	−1.21±0.12	0.27±0.06
320	−1.31±0.10	0.26±0.11	−1.28±0.14	0.30±0.06
340	−1.35±0.11	0.26±0.13	−1.34±0.16	0.32±0.07
360	−1.37±0.12	0.26±0.14	−1.41±0.17	0.35±0.08
380	−1.40±0.12	0.25±0.16	−1.47±0.19	0.37±0.09
400	−1.42±0.13	0.25±0.17	−1.52±0.21	0.40±0.10
420	−1.44±0.14	0.24±0.19	−1.57±0.23	0.42±0.11
440	−1.46±0.15	0.23±0.21	−1.63±0.25	0.45±0.12
460	−1.47±0.16	0.22±0.22	−1.67±0.27	0.47±0.12

obtained very similar (p,p) phase shifts[8] shows that form limiting is not an important factor. The (p,p) data are now complete enough to define a reliable scattering matrix over this entire energy range. Also, the fact that the over-all solution M value is close to its statistically predicted value of about 1 indicates that the experimenters have correctly evaluated the statistical uncertainties in their data.

Using the 26-parameter solution, we varied the pion-nucleon coupling constant g^2 to obtain the χ^2 (g^2) parabola. From this parabola we obtain $g^2=14.43\pm0.41$. All of our final solutions in this paper are quoted with this value for g^2 in calculating the OPE phases. With 24- and 28-parameter solutions, we obtained $g^2=14.24\pm0.40$ and $g^2=14.05\pm0.44$, respectively, which shows that a systematic variation of about 0.4 in g^2 is obtained by varying the particular choices for the phenomenological parameters.

Table IV gives the final (p,p) 26-parameter energy-dependent phases from 1 to 450 MeV. The errors on the phases are from the parameter error matrix. These errors should be interpreted as the *minimum* errors that

TABLE V. (n,p) data from 0.5 to 425 MeV. The data used in the final analyses are listed together with the M values and the normalization constants obtained from the $I=1$ solution of Table III combined with the 26-parameter experimental $I=0$ solution of Table VI. $\chi^2=1100$ for 990 (n,p) data, so the M value is 1.111. For the combined (p,p) plus (n,p) solution, $\chi^2=2226$ for 2066 data, so the combined M value is 1.077.

Energy (MeV)	Data	M value	Predicted norm.	Energy (MeV)	Data	M value	Predicted norm.	Energy (MeV)	Data	M value	Predicted norm.	Energy (MeV)	Data	M value	Predicted norm.
0.49	$1\sigma_T$	0.2		29.0	$1\sigma_T$	2.1		70.0	11σ	1.3	0.925	128.0	$1D_T$	0.0	
1.00	$1\sigma_T$	2.0		29.6	$1\sigma_T$	0.1	0.997	70.0	$9P$	1.4	0.927	128.5	$3A_T'$	1.6	
1.31	$1\sigma_T$	0.3		30.0	$9P$	1.2	0.970	70.0	$7P$	0.8	0.983	129.0	15σ	0.8	0.974
2.53	$1\sigma_T$	7.7		30.0	$3P$	1.3	0.969	72.0	$1\sigma_T$	2.3	0.980	129.4	$1\sigma_T$	0.8	
3.19	$1\sigma_T$	2.6		32.5	$1\sigma_T$	0.3	1.007	80.0	12σ	1.7	0.984	130.0	14σ	1.0	0.951
4.75	$1\sigma_T$	4.7		32.5	9σ	0.9	1.032	80.0	11σ	0.8	0.970	135.0	$5A$	0.7	0.997
7.17	$1\sigma_T$	0.6		32.5	6σ	1.2	0.978	80.0	$9P$	0.5	0.962	137.0	7σ	0.7	0.973
8.77	$1\sigma_T$	6.0		33.1	$1\sigma_T$	0.1	1.004	80.0	$7P$	0.6	1.025	137.0	$5R$	0.6	
10.42	$1\sigma_T$	1.3		34.0	$1\sigma_T$	0.2	0.994	82.8	$1\sigma_T$	2.0	0.980	140.0	$1\sigma_T$	0.8	
11.13	$1\sigma_T$	0.6		37.5	10σ	0.4	1.006	86.9	$1\sigma_T$	0.8	0.989	140.0	$14P$	1.7	1.079
13.13	$1\sigma_T$	0.9		37.5	7σ	0.7	0.961	88.0	$1\sigma_T$	1.1	1.016	140.9	$1\sigma_T$	1.6	
14.02	$1\sigma_T$	5.7		38.0	$1\sigma_T$	0.6	0.988	88.0	$1\sigma_T$	0.1	1.005	143.0	$8P$	1.5	0.901
14.1	8σ	0.4	0.952	38.5	$1\sigma_T$	0.2	0.994	88.0	$1\sigma_T$	2.7		150.0	16σ	0.6	0.982
14.1	16σ	0.2	0.976	40.0	$1\sigma_T$	0.0	1.002	89.5	13σ	1.3	0.979	150.9	$1\sigma_T$	1.6	
14.1	6σ	0.2	0.985	40.0	$9P$	0.9	1.084	89.5	11σ	1.0	0.963	153.0	$1\sigma_T$	5.2	0.971
14.1	4σ	5.7[a]	1.019	40.0	$6P$	0.7	1.051	90.0	$9P$	0.7	0.957	156.0	$1\sigma_T$	0.0	
14.1	$1\sigma_T$	0.5		41.1	$1\sigma_T$	0.5	0.991	90.0	$7P$	0.4	1.018	197.0	$3D_T$	1.1	
15.7	16σ	0.8	0.021	42.5	11σ	0.9	1.006	91.0	25σ	0.8	0.984	199.0	8σ	1.3	1.007
15.8–96	$22\sigma_T$	1.6		42.5	11σ	1.1	0.973	91.0	$1\sigma_T$	0.8	0.988	199.0	$8P$	1.1	0.963
16.1	$1\sigma_T$	0.1		42.5	$1\sigma_T$	0.6	0.990	95.0	$1\sigma_T$	0.6	0.993	200.0	20σ	1.6	1.004
16.4	$3P$	0.7	1.002	44.0	$1\sigma_T$	0.3	0.993	95.0	$15P$	2.1	0.955	200.0	$1\sigma_T$	0.0	
17.8	$1\sigma_T$	1.8		45.5	$1\sigma_T$	0.3	1.003	99.0	$1\sigma_T$	3.1		203.0	$5R_T$	0.8	0.967
18.4	$1\sigma_T$	0.4		45.5	$1\sigma_T$	0.2	1.005	99.0	13σ	1.4	0.985	212.0	$5D$	1.0	
19.6	$1\sigma_T$	0.5		47.5	11σ	1.1	1.015	99.0	11σ	1.1	1.020	217.0	$6P$	0.6	0.996
19.6	$1\sigma_T$	0.3		47.5	11σ	0.9	0.990	100.0	$9P$	0.4	1.037	260.0	15σ	1.9	0.975
20.5	$1\sigma_T$	0.6		48.8	$1\sigma_T$	0.2	0.994	100.0	$7P$	0.8	1.031	270.0	$1\sigma_T$	0.2	
20.5	$9P$	0.8	1.129	50.0	$9P$	0.5	1.053	100.0	$1\sigma_T$	0.0	0.998	290.0	3σ	0.1	1.024
20.6	$1\sigma_T$	0.0		50.0	$6P$	0.9	1.006	105.0	7σ	0.3	1.096	300.0	15σ	1.2	0.964
22.5	12σ	0.5	0.993	52.5	12σ	1.06	1.020	105.0	$1\sigma_T$	0.3	1.007	310.0	$19P$	0.8	1.012
22.5	6σ	0.6	0.981	52.5	11σ	0.8	1.018	108.5	13σ	1.5	0.992	310.0	$8P$	1.3	0.992
23.1	$6P$	1.0	0.940	52.5	$1\sigma_T$	0.3	0.993	108.5	11σ	1.8	1.014	350.0	$1\sigma_T$	0.6	
23.1	$1P$	4.3		56.6	$1\sigma_T$	0.0	1.003	110.0	$9P$	1.1	1.038	350.0	17σ	0.9	1.056
23.1	$4C_{NN}$	0.4		57.5	12σ	0.7	1.022	110.0	$7P$	1.4	1.058	350.0	$10P$	1.8	0.993
23.7	$1\sigma_T$	0.2		57.5	11σ	1.5	0.993	110.0	$1\sigma_T$	2.9		380.0	$1\sigma_T$	0.1	
23.7	$4P$	0.6	0.940	58.8	$1\sigma_T$	0.2	1.006	110.0	$1\sigma_T$	2.0	1.016	380.0	14σ	1.7	0.967
23.7	$1\sigma_T$	0.0		60.0	$9P$	0.9	0.951	120.0	$1\sigma_T$	1.8		400.0	21σ	1.5	1.004
24.0	4σ	1.6[b]	1.002	60.0	$7P$	1.8	0.977	120.0	$9P$	0.5	1.026	400.0	$8P$	3.7	1.040
25.3	$1\sigma_T$	2.5		62.5	12σ	1.4	0.997	120.0	$7P$	0.7	1.051	410.0	$1\sigma_T$	0.3	
25.9	$1\sigma_T$	0.9	1.009	62.5	11σ	1.3	0.952	126.0	$6P$	0.7	1.086	425.0	$3P$	7.7	1.047
27.5	8σ	0.1	1.001	63.0	$1\sigma_T$	0.6	1.007	126.0	$1\sigma_T$	0.3	0.996	425.0	$3D$	0.3	
27.5	3σ	0.9	0.925	66.1	$1\sigma_T$	0.1	0.995	128.0	10σ	0.3	0.999	425.0	$3R$	1.0	
28.0	$1\sigma_T$	5.5		68.9	$1\sigma_T$	0.1	0.996	128.0	$10P$	1.6	1.046	425.0	$3A$	0.8	
28.3	$1\sigma_T$	1.3		70.0	12σ	1.5	1.004	128.0	$5D_T$	1.9					

[a] $M=1.6$ for the solution from Table VII. [b] $M=0.1$ for the solution from Table VII.

are statistically allowed by the uncertainties in the *total body of* (p,p) *experimental data*. They would be the true errors if our energy-dependent forms could be shown to be exact. The errors on the energy-independent analyses, which are discussed in Sec. VII, should be interpreted as the *maximum* errors that are statistically allowed by the (p,p) *data in each energy band*. They would be the true errors if the phase shifts in one energy band were completely unrelated to the phases in adjacent energy bands. Since this is obviously not correct (as shown by both the Yale and the Livermore energy-dependent results), the true errors must lie somewhere in between.

V. (n,p) ENERGY-DEPENDENT ANALYSES

In Paper IX we described an energy-dependent (p,p) plus (n,p) phase-shift analysis. This analysis was carried out by using (p,p) data to determine the $I=1$ scattering matrix, and then using the $I=1$ matrix plus the (n,p) data to determine the $I=0$ scattering matrix. In the present paper we followed the same procedure to determine the $I=0$ scattering matrix, but with one notable exception: a separate (n,p) $^1S_0$ phase was assigned in addition to the $I=0$ phases in fitting to the (n,p) data. The desirability for this charge-dependent effect was pointed out by the Yale group,[8] and the necessity was indicated by our difficulty[3] in fitting to (n,p) total cross sections when we did not include this effect. The $I=1$ scattering matrix (Table IV) had been determined by fitting to 1076 (p,p) data from 1.39 to 450 MeV. The $I=0$ scattering matrix was determined by fitting to 990 (n,p) data from 0.49 to 425 MeV. Thus the combined $I=1$ plus $I=0$ matrices represent a fit to 2066 (p,p) and (n,p) data extending from 0.49to 450 MeV.

TABLE VI. (n,p) phase shifts for the 52-parameter energy-dependent combined (p,p) plus (n,p) experimental solution. The $I=1$ phases except for $^1S_0$, are those of Table IV. The χ^2 value for the fit to 990 data is 1100 for this solution. The data are described in Table V'

Energy (MeV)	$^1S_0$ (n,p)	$^1P_1$	$^1F_3$	$^1H_5$	$^3S_1$
1	62.43±0.01	−0.12±0.01	−0.00±0.00	−0.00±0.00	147.85±0.01
2	65.03±0.03	−0.29±0.02	−0.00±0.00	−0.00±0.00	136.55±0.02
3	65.35±0.06	−0.46±0.04	−0.00±0.00	−0.00±0.00	128.83±0.03
4	65.06±0.08	−0.62±0.06	−0.01±0.00	−0.00±0.00	122.92±0.05
5	64.53±0.11	−0.77±0.07	−0.01±0.00	−0.00±0.00	118.12±0.07
6	63.91±0.14	−0.90±0.09	−0.02±0.00	−0.00±0.00	114.07±0.09
8	63.57±0.20	−1.11±0.13	−0.04±0.00	−0.00±0.00	107.49±0.13
10	61.23±0.26	−1.27±0.17	−0.07±0.00	−0.00±0.00	102.22±0.16
12	59.95±0.32	−1.39±0.21	−0.11±0.00	−0.00±0.00	97.84±0.20
14	58.73±0.37	−1.48±0.25	−0.16±0.00	−0.01±0.00	94.07±0.23
16	57.56±0.42	−1.54±0.29	−0.21±0.00	−0.01±0.00	90.78±0.26
18	56.46±0.47	−1.61±0.31	−0.26±0.01	−0.01±0.00	87.84±0.29
20	55.41±0.52	−1.68±0.34	−0.31±0.01	−0.02±0.00	85.18±0.32
25	52.96±0.62	−1.85±0.39	−0.45±0.01	−0.04±0.00	79.48±0.38
30	50.73±0.71	−2.07±0.44	−0.59±0.02	−0.06±0.00	74.76±0.41
40	46.72±0.86	−2.75±0.49	−0.87±0.04	−0.12±0.00	67.19±0.46
50	43.16±0.98	−3.74±0.52	−1.13±0.06	−0.19±0.00	61.20±0.47
60	39.90±1.10	−4.97±0.53	−1.35±0.09	−0.27±0.00	56.21±0.47
70	36.89±1.21	−6.38±0.54	−1.54±0.12	−0.36±0.00	51.90±0.45
80	34.08±1.33	−7.91±0.55	−1.71±0.15	−0.46±0.01	48.08±0.44
90	31.45±1.44	−9.49±0.57	−1.85±0.18	−0.56±0.01	44.62±0.42
100	28.97±1.55	−11.10±0.59	−1.98±0.21	−0.65±0.02	41.43±0.42
120	24.41±1.74	−14.27±0.65	−2.18±0.27	−0.86±0.03	35.67±0.43
140	20.31±1.88	−17.26±0.72	−2.35±0.31	−1.07±0.04	30.48±0.46
160	16.62±1.97	−19.99±0.79	−2.48±0.35	−1.28±0.06	25.68±0.50
180	13.27±2.02	−22.42±0.85	−2.61±0.38	−1.49±0.08	21.17±0.54
200	10.22±2.04	−24.55±0.92	−2.72±0.41	−1.71±0.11	16.89±0.58
220	7.45±2.02	−26.38±0.99	−2.83±0.43	−1.92±0.13	12.78±0.63
240	4.92±2.00	−27.92±1.08	−2.94±0.46	−2.14±0.16	8.83±0.69
260	2.61±1.97	−29.21±1.19	−3.06±0.50	−2.36±0.19	5.02±0.76
280	0.49±1.96	−30.24±1.32	−3.18±0.54	−2.57±0.22	1.33±0.85
300	−1.46±1.98	−31.06±1.48	−3.30±0.59	−2.79±0.26	−2.25±0.95
320	−3.25±2.04	−31.67±1.65	−3.43±0.66	−3.01±0.29	−5.73±1.06
340	−4.90±2.16	−32.09±1.84	−3.56±0.74	−3.22±0.33	−9.11±1.19
360	−6.41±2.32	−32.35±2.04	−3.70±0.82	−3.44±0.37	−12.40±1.34
380	−7.81±2.53	−32.46±2.26	−3.85±0.92	−3.65±0.40	−15.61±1.49
400	−9.10±2.78	−32.43±2.50	−4.00±1.03	−3.86±0.44	−18.73±1.65
420	−10.29±3.07	−32.28±2.74	−4.15±1.14	−4.07±0.48	−21.76±1.82
440	−11.39±3.39	−32.02±2.99	−4.31±1.26	−4.28±0.52	−24.72±2.00
460	−12.41±3.73	−31.65±3.24	−4.47±1.39	−4.49±0.56	−27.61±2.19

Energy (MeV)	ϵ_1	$^3D_1$	$^3D_2$	$^3D_3$	ϵ_3
1	−0.01±0.01	−0.00±0.00	0.01±0.00	0.00±0.00	0.00±0.00
2	−0.04±0.02	−0.02±0.00	0.04±0.00	0.00±0.00	0.00±0.00
3	−0.07±0.04	−0.05±0.00	0.09±0.00	0.00±0.00	0.00±0.00
4	−0.10±0.06	−0.09±0.00	0.16±0.00	0.00±0.00	0.01±0.00
5	−0.14±0.07	−0.15±0.00	0.26±0.00	0.01±0.00	0.02±0.00
6	−0.18±0.10	−0.22±0.01	0.37±0.00	0.01±0.00	0.03±0.00
8	−0.24±0.14	−0.38±0.01	0.65±0.00	0.02±0.00	0.05±0.00
10	−0.31±0.18	−0.58±0.02	0.97±0.01	0.03±0.01	0.09±0.00
12	−0.38±0.22	−0.81±0.02	1.33±0.01	0.04±0.01	0.14±0.00
14	−0.44±0.25	−1.05±0.03	1.73±0.02	0.06±0.01	0.20±0.00
16	−0.51±0.28	−1.31±0.04	2.14±0.02	0.07±0.01	0.26±0.00
18	−0.55±0.32	−1.58±0.05	2.58±0.02	0.10±0.02	0.33±0.00
20	−0.59±0.35	−1.86±0.06	3.02±0.03	0.12±0.02	0.40±0.00
25	−0.68±0.42	−2.60±0.09	4.16±0.05	0.18±0.03	0.60±0.00
30	−0.72±0.47	−3.35±0.11	5.32±0.07	0.25±0.04	0.81±0.00
40	−0.69±0.53	−4.84±0.16	7.59±0.10	0.42±0.07	1.25±0.01
50	−0.54±0.56	−6.28±0.19	9.76±0.14	0.62±0.10	1.67±0.01
60	−0.28±0.56	−7.63±0.21	11.76±0.18	0.83±0.13	2.07±0.02
70	0.05±0.55	−8.88±0.23	13.60±0.22	1.04±0.15	2.44±0.03
80	0.45±0.53	−10.03±0.24	15.26±0.25	1.25±0.18	2.78±0.04
90	0.89±0.52	−11.08±0.25	16.76±0.28	1.45±0.20	3.09±0.06
100	1.38±0.50	−12.05±0.25	18.10±0.30	1.64±0.22	3.37±0.07
120	2.41±0.49	−13.73±0.29	20.36±0.34	1.97±0.25	3.85±0.10
140	3.51±0.49	−15.14±0.33	22.10±0.36	2.25±0.27	4.25±0.13
160	4.63±0.51	−16.32±0.38	23.40±0.39	2.46±0.29	4.57±0.17
180	5.75±0.53	−17.30±0.43	24.34±0.41	2.62±0.31	4.84±0.20
200	6.86±0.56	−18.12±0.48	24.96±0.44	2.72±0.33	5.05±0.24
220	7.94±0.58	−18.82±0.51	25.31±0.48	2.77±0.35	5.22±0.28

TABLE VI. (*continued*).

Energy (MeV)	ϵ_1	$^3D_1$	$^3D_2$	$^3D_3$	ϵ_3
240	9.00±0.60	−19.40±0.53	25.43±0.53	2.77±0.37	5.36±0.32
260	10.03±0.63	−19.90±0.56	25.37±0.59	2.74±0.40	5.48±0.35
280	11.02±0.68	−20.31±0.58	25.14±0.66	2.67±0.43	5.56±0.39
300	11.98±0.73	−20.67±0.62	24.77±0.74	2.56±0.47	5.63±0.43
320	12.91±0.80	−20.97±0.68	24.28±0.82	2.43+0.51	5.68±0.46
340	13.80±0.89	−21.22±0.76	23.69±0.92	2.27±0.56	5.72±0.50
360	14.66±0.98	−21.44±0.87	23.02±1.01	2.10±0.61	5.74±0.54
380	15.48±1.10	−21.63±1.01	22.27±1.12	1.90±0.66	5.76±0.57
400	16.27±1.22	−21.79±1.17	21.47±1.22	1.68±0.72	5.76±0.61
420	17.04±1.35	−21.92±1.35	20.61±1.33	1.45±0.78	5.76±0.64
440	17.77±1.49	−22.04±1.55	19.70±1.44	1.21±0.84	5.75±0.67
460	18.47±1.64	−22.14±1.76	18.77±1.55	0.95±0.90	5.74±0.70

Energy (MeV)	$^3G_3$	$^3G_4$	$^3G_5$
1	−0.00±0.00	0.00±0.00	−0.00±0.00
2	−0.00±0.00	0.00±0.00	−0.00±0.00
3	−0.00±0.00	0.00±0.00	−0.00±0.00
4	−0.00±0.00	0.00±0.00	−0.00±0.00
5	−0.00±0.00	0.00±0.00	−0.00±0.00
6	−0.00±0.00	0.00±0.00	−0.00±0.00
8	−0.00±0.00	0.01±0.01	−0.00±0.00
10	−0.00±0.00	0.02±0.00	−0.00±0.00
12	−0.01±0.00	0.03±0.00	−0.00±0.00
14	−0.01±0.00	0.04±0.00	−0.00±0.00
16	−0.02±0.00	0.06±0.00	−0.00±0.00
18	−0.03±0.00	0.09±0.00	−0.00±0.00
20	−0.04±0.00	0.11±0.00	−0.01±0.00
25	−0.07±0.00	0.19±0.00	−0.01±0.00
30	−0.10±0.00	0.29±0.00	−0.02±0.00
40	−0.20±0.00	0.52±0.00	−0.04±0.00
50	−0.32±0.01	0.79±0.01	−0.07±0.00
60	−0.46±0.01	1.08±0.01	−0.10±0.01
70	−0.62±0.02	1.37±0.02	−0.14±0.01
80	−0.79±0.03	1.67±0.03	−0.19±0.02
90	−0.97±0.04	1.97±0.04	−0.23±0.02
100	−1.17±0.05	2.27±0.05	−0.28±0.03
120	−1.58±0.08	2.85±0.08	−0.39±0.05
140	−2.01±0.11	3.41±0.12	−0.50±0.07
160	−2.47±0.15	3.95±0.16	−0.61±0.09
180	−2.94±0.20	4.47±0.21	−0.72±0.11
200	−3.42±0.24	4.96±0.26	−0.83±0.14
220	−3.90±0.29	5.43±0.31	−0.94±0.17
240	−4.39±0.34	5.88±0.36	−1.05±0.20
260	−4.88±0.40	6.31±0.42	−1.16±0.23
280	−5.37±0.45	6.72±0.48	−1.27±0.26
300	−5.85±0.51	7.11±0.54	−1.37±0.29
320	−6.34±0.56	7.49±0.60	−1.48±0.32
340	−6.82±0.62	7.85±0.66	−1.58±0.36
360	−7.29±0.68	8.20±0.72	−1.68±0.39
380	−7.76±0.74	8.53±0.78	−1.78±0.42
400	−8.22±0.79	8.85±0.84	−1.87±0.46
420	−8.68±0.85	9.16±0.90	−1.97±0.49
440	−9.14±0.91	9.46±0.96	−2.06±0.52
460	−9.58±0.97	9.75±1.02	−2.15±0.56

As in the (p,p) analyses described above, we investigated different choices for the number of free parameters to be assigned to the $I=0$ phases. In our previous work,[3] we chose a 22-parameter representation. In the present work, we finally selected a representation that uses 23 parameters for the $I=0$ phases plus three parameters for the (n,p) $^1S_0$ phase (no inelasticity was assigned to these phases). With these 26 phenomenological parameters, and holding the $I=1$ scattering matrix fixed as shown in Table IV, we obtained a solution having a χ^2 sum of 1100, and thus an M value of 1.111, for the fit to the 990 (n,p) data. Table V gives the data list for this solution, and the M values and normalization constants for the separate data sets. The Kyoto[15] and Wisconsin[16] data are included. Table VI gives the phase shifts, with errors as obtained from the parameter error matrix.

Tables IV and VI, taken together, represent a combined fit to 1076 (p,p) data and 990 (n,p) data, or 2066 data in all. A total of 52 phenomenological

TABLE VII. (n,p) phase shifts for the 52-parameter energy-dependent combined (p,p) plus (n,p) *constrained* solution. This solution is similar to that of Table VI except for ϵ_1 and $^1P_1$ phases at low energies. The χ^2 value for the fit to the (n,p) data is 1138.

Energy (MeV)	$^1S_0$ (n,p)	$^1P_1$	$^1F_3$	$^1H_5$	$^3S_1$
1	62.41±0.01	−0.17±0.00	−0.00±0.00	−0.00±0.00	147.84±0.01
2	64.97±0.03	−0.43±0.00	−0.00±0.00	−0.00±0.00	136.54±0.02
3	65.26±0.06	−0.71±0.01	−0.00±0.00	−0.00±0.00	128.81±0.03
4	64.93±0.08	−1.00±0.01	−0.01±0.00	−0.00±0.00	122.89±0.05
5	64.35±0.11	−1.28±0.01	−0.01±0.00	−0.00±0.00	118.08±0.07
10	60.85±0.26	−2.46±0.03	−0.07±0.00	−0.00±0.00	102.12±0.16
14	58.22±0.37	−3.18±0.04	−0.15±0.00	−0.01±0.00	93.92±0.23
20	54.79±0.52	−4.03±0.06	−0.30±0.01	−0.02±0.00	84.94±0.31
25	52.31±0.62	−4.61±0.08	−0.43±0.01	−0.04±0.00	79.18±0.37
30	50.10±0.71	−5.14±0.10	−0.56±0.02	−0.06±0.00	74.41±0.41
40	46.29±0.86	−6.16±0.17	−0.81±0.04	−0.12±0.00	66.73±0.46
50	43.02±0.98	−7.19±0.24	−1.03±0.06	−0.19±0.00	60.67±0.47
60	40.14±1.10	−8.27±0.32	−1.20±0.09	−0.27±0.00	55.63±0.46
70	37.54±1.22	−9.40±0.40	−1.34±0.11	−0.36±0.00	51.30±0.45
80	35.15±1.34	−10.55±0.47	−1.46±0.14	−0.45±0.01	47.47±0.44
90	32.92±1.46	−11.72±0.54	−1.55±0.17	−0.55±0.01	44.02±0.42
100	30.83±1.57	−12.90±0.59	−1.62±0.20	−0.65±0.02	40.86±0.42
120	26.94±1.77	−15.23±0.69	−1.73±0.25	−0.85±0.03	35.18±0.43
140	23.37±1.92	−17.47±0.76	−1.81±0.29	−1.05±0.04	30.11±0.46
160	20.04±2.02	−19.59±0.82	−1.89±0.33	−1.25±0.06	25.46±0.50
180	16.92±2.08	−21.57±0.88	−1.96±0.36	−1.46±0.08	21.11±0.54
200	13.96±2.10	−23.41±0.95	−2.04±0.39	−1.66±0.10	17.01±0.59
220	11.14±2.10	−25.10±1.03	−2.14±0.42	−1.87±0.13	13.11±0.65
240	8.45±2.07	−26.65±1.13	−2.26±0.45	−2.07±0.16	9.36±0.72
260	5.89±2.05	−28.07±1.26	−2.39±0.49	−2.27±0.19	5.76±0.80
280	3.43±2.03	−29.36±1.41	−2.54±0.54	−2.48±0.22	2.28±0.91
300	1.06±2.05	−30.54±1.58	−2.71±0.59	−2.68±0.26	−1.09±1.03
320	−1.21±2.11	−31.60±1.77	−2.90±0.66	−2.88±0.29	−4.35±1.17
340	−3.39±2.21	−32.56±1.97	−3.10±0.74	−3.08±0.33	−7.52±1.33
360	−5.49±2.36	−33.43±2.19	−3.32±0.83	−3.28±0.36	−10.60±1.50
380	−7.52±2.55	−34.21±2.41	−3.56±0.92	−3.47±0.40	−13.59±1.68
400	−9.48±2.79	−34.91±2.64	−3.81±1.03	−3.67±0.44	−16.50±1.87
420	−11.37±3.07	−35.53±2.87	−4.07±1.14	−3.86±0.48	−19.33±2.06
440	−13.19±3.37	−36.09±3.11	−4.34±1.26	−4.05±0.52	−22.09±2.27
460	−14.95±3.70	−36.58±3.35	−4.63±1.38	−4.24±0.56	−24.77±2.48

Energy (MeV)	ϵ_1	$^3D_1$	$^3D_2$	$^3D_3$	ϵ_3
1	0.02±0.01	−0.00±0.00	0.01±0.00	0.00±0.00	0.00±0.00
2	0.06±0.02	−0.02±0.00	0.04±0.00	0.00±0.00	0.00±0.00
3	0.11±0.03	−0.05±0.00	0.09±0.00	0.00±0.00	0.00±0.00
4	0.16±0.04	−0.09±0.00	0.16±0.00	0.01±0.00	0.01±0.00
5	0.22±0.06	−0.14±0.00	0.26±0.00	0.01±0.00	0.02±0.00
10	0.51±0.14	−0.55±0.02	0.96±0.01	0.04±0.00	0.09±0.00
14	0.75±0.19	−0.99±0.03	1.71±0.02	0.07±0.01	0.20±0.00
20	1.06±0.27	−1.74±0.06	2.97±0.03	0.15±0.02	0.40±0.00
25	1.29±0.32	−2.42±0.08	4.08±0.05	0.23±0.03	0.60±0.00
30	1.49±0.36	−3.12±0.11	5.21±0.07	0.32±0.04	0.81±0.00
40	1.81±0.41	−4.52±0.15	7.43±0.11	0.54±0.07	1.25±0.01
50	2.06±0.44	−5.88±0.18	9.53±0.16	0.78±0.09	1.67±0.01
60	2.27±0.45	−7.17±0.20	11.48±0.20	1.04±0.12	2.07±0.02
70	2.47±0.45	−8.39±0.22	13.26±0.23	1.30±0.14	2.44±0.03
80	2.66±0.45	−9.54±0.23	14.89±0.27	1.55±0.16	2.77±0.04
90	2.86±0.45	−10.60±0.24	16.35±0.30	1.80±0.18	3.08±0.06
100	3.08±0.45	−11.59±0.25	17.67±0.32	2.02±0.20	3.36±0.07
120	3.57±0.46	−13.35±0.28	19.90±0.36	2.43±0.23	3.84±0.10
140	4.15±0.48	−14.86±0.33	21.64±0.39	2.76±0.26	4.23±0.13
160	4.82±0.49	−16.14±0.38	22.98±0.41	3.01±0.28	4.55±0.17
180	5.58±0.51	−17.22±0.43	23.98±0.44	3.20±0.30	4.81±0.20
200	6.42±0.53	−18.12±0.48	24.68±0.47	3.32±0.32	5.02±0.24
220	7.32±0.56	−18.87±0.51	25.13±0.51	3.38±0.34	5.19±0.28
240	8.26±0.59	−19.49±0.54	25.37±0.56	3.39±0.37	5.32±0.31
260	9.27±0.63	−19.99±0.56	25.42±0.63	3.35±0.40	5.43±0.35
280	10.30±0.68	−20.39±0.59	25.33±0.70	3.26±0.44	5.51±0.39
300	11.37±0.76	−20.70±0.63	25.11±0.79	3.14±0.48	5.58±0.43
320	12.46±0.84	−20.92±0.68	24.77±0.88	2.99±0.53	5.62±0.46
340	13.56±0.94	−21.08±0.75	24.34±0.98	2.80±0.57	5.65±0.50
360	14.68±1.05	−21.17±0.85	23.83±1.09	2.59±0.63	5.67±0.53
380	15.80±1.18	−21.21±0.97	23.25±1.20	2.36±0.68	5.68±0.57
400	16.93±1.31	−21.20±1.11	22.61±1.31	2.11±0.74	5.69±0.60
420	18.05±1.45	−21.14±1.28	21.92±1.43	1.84±0.80	5.68±0.64

TABLE VII. (*continued*).

Energy (MeV)	ϵ_1	$^3D_1$	$^3D_2$	$^3D_3$	ϵ_3
440	19.18±1.59	−21.05±1.46	21.19±1.55	1.56±0.85	5.67±0.67
460	20.30±1.74	−20.92±1.66	20.43±1.67	1.26±0.91	5.65±0.70

Energy (MeV)	$^3G_3$	$^3G_4$	$^3G_5$
1	−0.00±0.00	0.00±0.00	−0.00±0.00
2	−0.00±0.00	0.00±0.00	−0.00±0.00
3	−0.00±0.00	0.00±0.00	−0.00±0.00
4	−0.00±0.00	0.00±0.00	−0.00±0.00
5	−0.00±0.00	0.00±0.00	−0.00±0.00
10	−0.00±0.00	0.02±0.00	−0.00±0.00
14	−0.01±0.00	0.04±0.00	−0.00±0.00
20	−0.04±0.00	0.11±0.00	−0.01±0.00
25	−0.07±0.00	0.19±0.00	−0.01±0.00
30	−0.10±0.00	0.29±0.00	−0.02±0.00
40	−0.20±0.00	0.52±0.00	−0.04±0.00
50	−0.31±0.01	0.79±0.01	−0.07±0.00
60	−0.45±0.01	1.07±0.01	−0.10±0.01
70	−0.60±0.02	1.36±0.02	−0.14±0.01
80	−0.77±0.03	1.66±0.03	−0.18±0.02
90	−0.94±0.04	1.96±0.04	−0.22±0.02
100	−1.12±0.05	2.26±0.06	−0.27±0.03
120	−1.51±0.08	2.84±0.09	−0.36±0.05
140	−1.92±0.11	3.39±0.13	−0.46±0.07
160	−2.34±0.15	3.93±0.17	−0.56±0.09
180	−2.78±0.19	4.43±0.22	−0.65±0.11
200	−3.22±0.24	4.92±0.27	−0.75±0.14
220	−3.66±0.29	5.38±0.33	−0.85±0.17
240	−4.11±0.34	5.82±0.39	−0.94±0.20
260	−4.55±0.39	6.23±0.45	−1.03±0.23
280	−5.00±0.44	6.63±0.51	−1.12±0.26
300	−5.44±0.50	7.02±0.57	−1.21±0.30
320	−5.87±0.55	7.38±0.64	−1.29±0.33
340	−6.31±0.61	7.73±0.70	−1.38±0.36
360	−6.73±0.66	8.07±0.77	−1.46±0.40
380	−7.16±0.72	8.39±0.83	−1.54±0.43
400	−7.57±0.78	8.71±0.90	−1.61±0.47
420	−7.98±0.83	9.01±0.96	−1.69±0.50
440	−8.39±0.89	9.29±1.03	−1.76±0.53
460	−8.79±0.95	9.57±1.09	−1.83±0.57

parameters are used to represent the phase shifts, and the χ^2 sum for the combined solution is 2226. Thus the over-all M value is 1.077.

The expected χ^2 value for 2066 data and 52 adjustable parameters is 2014 if the data are consistent and the experimenters have estimated their errors correctly. The value we obtain (2226) is close enough to this value to indicate that the data are quite consistent, and that the standard deviations quoted are realistic. It also indicates that the energy-dependent parametrization is a good one, since the 52 parameters are sufficient to give adequate freedom to the 28 phase shifts over the entire energy span from 0.5 to 450 MeV. Adding additional parameters does not significantly lower the over-all χ^2, and it eventually leads to a numerically undefined error matrix for the parameters.

One problem that arises in connection with the $I=0$ phases of Table VI concerns the energy dependence of the ϵ_1 and $^1P_1$ phases. As can be seen in Table VI, the ϵ_1 phase has negative values below 80 MeV. From the sign of the quadrupole moment of the deuteron, we expect ϵ_1 to be positive at low energies.[17] Hence our negative value for ϵ_1 would seem to be a reflection of the inadequacy of the (n,p) data collection below 80 MeV. Also, the $^1P_1$ phase, which might be expected to approximate the OPE phase shift at low energies, actually assumes a much smaller value.[18]

To further investigate this difficulty, we first made a modification in the (n,p) analysis that offers one solution (a rather arbitrary one) to the difficulty, and that also clarifies the nature of the problem. We constrained the ϵ_1 phase to remain positive (by adding in ϵ_1 "pseudo-data" to the χ^2 calculation at three energies). When a solution was thus obtained that had a positive ϵ_1 at low energies, we discovered that the $^1P_1$ phase simultaneously changed and assumed values much closer to the OPE values. Thus the ambiguity in the $I=0$ phases at low energies exists because the $^1P_1$ and ϵ_1 phases exhibit a strong correlation that is not delineated by the existing low-energy (n,p) data.

When the new Wisconsin data[16] became available, we used these to obtain a second constrained solution

[18] We thank J. Simmons, J. Hopkins, and P. Signell for useful discussions on this point.

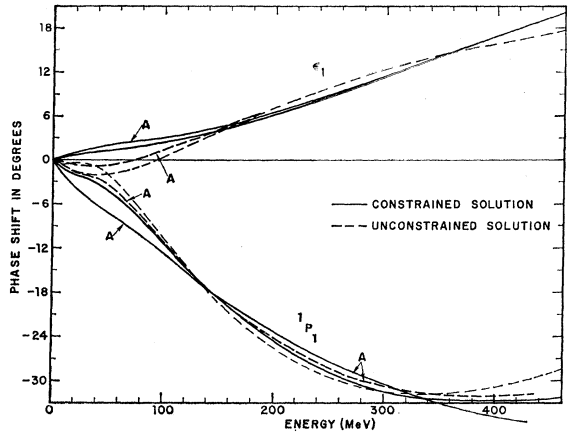

FIG. 1. ϵ_1 and $^1P_1$ phase shifts for the unconstrained and constrained isotopic-spin-0 solutions. The unconstrained solution has values for ϵ_1 and $^1P_1$ that are in disagreement with theoretical expectations at low energies. When we constrain ϵ_1 to remain positive at low energies, then $^1P_1$ also moves out to the larger (negative) values predicted from OPE. The curves labeled *A* are for the solutions given in Tables VI and VII; these are the results after the addition of the Wisconsin and Kyoto data, as discussed in the text. The other curves are the corresponding solutions before the addition of the Wisconsin and Kyoto data, as also discussed in the text.

by forcing an exact fit to the ratlo $\sigma(165°)/\sigma(89°) = 1.134$, as measured for (n,p) scattering at 24 MeV.[16] [The accuracy of the experimental measurement was 2%. The unconstrained solution of Table VI gave a ratio of 1.084, which is $2\frac{1}{2}$ standard deviations lower than the measured value. This indicates some inconsistency among the (n,p) data.] This second constrained solution has ϵ_1 and $^1P_1$ phases that are in reasonable agreement with theoretical expectations.[17,18] This solution is given in Table VII. The χ^2 sum for this solution is 1138 as against a value of 1100 for the unconstrained solution of Table VI. Thus the constrained solution, statistically speaking, is still an excellent fit to the data. Some workers might prefer to use this solution instead of the one in Table VI because the phases are more in line with theoretical expectations. Figure 1 shows the behavior of the ϵ_1 and $^1P_1$ phases for the solutions that we have discussed here.

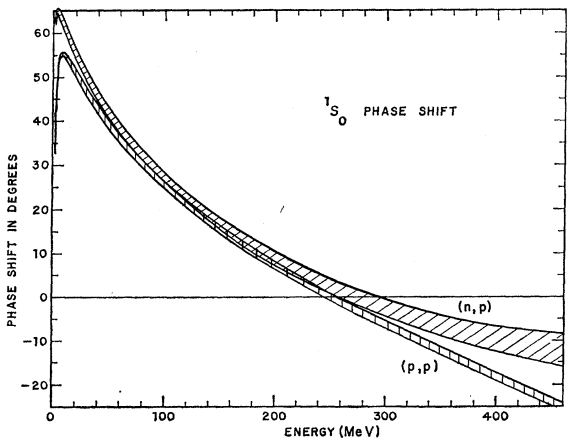

FIG. 2. The $^1S_0(p,p)$ and $^1S_0(n,p)$ phase shifts. The splitting at low energies, caused by two different effective-range extrapolations, is just right to give precise fits to the low-energy (p,p) and (n,p) data. The splitting above 200 MeV may be anomalous. The error bands shown, which are taken from the energy-dependent values of Tables IV and VI, should be regarded as the *minimum* uncertainties in the phases.

In an effort to see if we should include charge-dependent effects in any phases besides $^1S_0$, we tried searches in which first $^1D_2$ and then $^3P_0$ were given separate (n,p) parameters. These indicated that, given the existing body of (p,p) and (n,p) data, significant charge-dependent effects exist only in the $^1S_0$ phase. Figure 2 shows the splitting of the (p,p) and (n,p) phase shifts.

Experiments needed to remove the ambiguity in the low-energy ϵ_1 and $^1P_1$ phases were investigated in detail by comparing predictions of the observables for the two energy-dependent solutions listed in Tables VI and VII. As we have shown in Fig. 1, the ϵ_1 and $^1P_1$ uncertainties at low energies are highly correlated. Comparing predicted observables for these two solutions, we found that the (n,p) P, D, R, A, R', A', C_{KP}, A_{ZX}, C_{NKP}, C_{PNP}, and C_{KNP} predictions are almost identical. The values predicted for C_{NN} at 25 MeV differ by a factor of 2 for the unconstrained and constrained solutions over the angular range 0°–~90°. At the back angles, where (n,p) C_{NN} measurements exist,[19] the two solutions have very similar predictions. A measurement of the (n,p) C_{NN} observable at 45° c.m. to an accuracy of ± 0.02 would distinguish between the two solutions. This is not an easy experiment. The D_T, A_T, R_T', A_T', C_{KK}, C_{PP}, A_{ZZ}, and A_{XX} observables at 25 MeV all have differences in certain angular regions, but in each case an absolute precision of ± 0.02 to ± 0.04 is required to distinguish between solutions.

The one reasonable experiment to carry out in removing the (n,p) solution ambituity is the simplest one—a measurement of the (n,p) differential cross section. A solution having a large (negative) $^1P_1$ phase (the constrained solution of Table VII) has a slightly more asymmetric (n,p) differential cross section than does a solution having a small (negative) $^1P_1$ phase (Table VI).[18] The effect is not large, but it is measurable. The recent Wisconsin measurement,[16] which has an accuracy of about 2%, and the Kyoto measurement,[15] with about the same accuracy, are helpful in reducing the solution ambiguity. Unfortunately these data are somewhat at variance with other (n,p) data, as indicated by the results of the phase-shift analyses. In this situation additional measurements of the 180°/90° ratio for (n,p) differential scattering below 60 MeV would be very useful. To have much influence on the analysis, these data would have to have an accuracy of at least 2%.

[19] J. J. Malanify, P. J. Bendt, T. R. Roberts, and J. E. Simmons, Phys. Rev. Letters **17**, 481 (1966); and private communication from the authors.

TABLE VIII. Energy-independent solutions for combined (p,p) plus (n,p) data.

Energy (MeV)	25	50	95	142	210	330	425
(p,p) data	43	98	102	187	65	136	116
(n,p) data	87	107	59	119	56	73	48
Total data	130	205	161	305	121	209	164
χ^2	80.99	179.3	142.1	303.0	94.6	181.3	190.1
Energy band (MeV)	20.2–30	47.5–60	95–100	128–156	197–217	290–350	400–437
$^1S_0$ (p,p)	48.60±0.26	39.43±0.44	25.53±1.09	16.70±0.54	5.42±0.53	−10.53±1.33	−19.00±1.61
$^1D_2$	0.74±0.03	1.67±0.10	3.71±0.24	5.11±0.16	7.05±0.28	9.26±0.46	11.67±0.89
$^1G_4$				0.62±0.06	1.00±0.10	1.22±0.23	1.96±0.34
$^3P_0$	8.52±0.31	10.58±0.66	10.95±1.94	6.29±0.49	−0.86±0.56	−12.52±1.59	−16.70±1.83
$^3P_1$	−5.04±0.15	−8.39±0.29	−13.68±0.45	−17.04±0.16	−22.22±0.32	−28.79±1.19	−34.39±1.21
$^3P_2$	2.45±0.08	5.76±0.14	10.08±0.34	13.68±0.10	15.67±0.23	16.25±0.55	19.04±0.91
ϵ_2		−1.63±0.19	−2.63±0.25	−2.86±0.07	−2.82±0.16	−2.56±0.41	−0.96±0.65
$^3F_2$		−0.02±0.28	1.19±0.61	0.65±0.23	1.16±0.33	0.49±0.57	1.46±0.75
$^3F_3$		−0.38±0.37	−0.91±0.49	−2.05±0.16	−2.58±0.20	−3.58±0.58	−3.25±0.59
$^3F_4$		0.21±0.15	0.89±0.19	0.90±0.12	2.02±0.19	2.77±0.23	3.34±0.54
ϵ_4				−0.68±0.03	−0.99±0.09	−1.11±0.28	−2.19±0.34
$^3H_4$					0.24±0.21	1.12±0.32	−0.32±0.45
$^3H_5$					−1.07±0.18	−1.80±0.46	−1.90±0.43
$^3H_6$					0.15±0.13	0.77±0.15	0.03±0.32
$^1S_0$ (n,p)	48.84±1.75	54.66±8.99	35.48±10.18	20.42±4.12	3.09±4.94	(−10.53)	(−19.00)
$^1P_1$	−4.00±0.69	−1.34±1.71	−10.83±2.88	−18.22±1.33	−22.36±2.74	−26.11±8.95	−23.98±2.81
$^1F_3$				−2.02±0.79	−4.80±0.86	−6.37±4.02	−4.91±1.05
$^1H_5$						−1.89±1.49	−5.28±0.90
$^3S_1$	84.49±2.70	57.11±2.69	44.98±3.10	29.33±0.93	13.85±1.50	−11.21±4.43	−24.85±2.37
ϵ_1	−0.34±0.73	3.53±3.27	−1.28±3.79	4.28±0.96	6.47±0.70	20.69±5.53	16.07±1.68
$^3D_1$	−3.21±0.18	−5.28±1.80	−10.62±1.34	−14.44±0.78	−17.94±1.49	−21.28±1.70	−24.09±1.97
$^3D_2$		9.36±2.24	12.32±3.23	22.54±0.79	27.31±1.23	23.62±3.04	18.42±2.09
$^3D_3$		1.50±0.94	3.22±1.22	2.52±0.64	3.67±1.01	2.99±1.19	−1.22±1.45
ϵ_3				4.44±0.40	6.70±0.36	3.94±1.28	4.12±1.23
$^3G_3$						−6.07±1.91	−9.30±1.35
$^3G_4$						11.24±2.16	11.08±1.08
$^3G_5$						0.22±0.66	−1.82±0.78

VI. ENERGY-INDEPENDENT ANALYSES

Energy-independent solutions for combined (p,p) plus (n,p) data in narrow energy bands were obtained at 25, 50, 95, 142, 210, 330, and 425 MeV. Of the 2066 data used for the combined energy-dependent analysis, a total of 1296 data were included in the single-energy analyses. The data and phase-shift values are summarized in Table VIII.

In carrying out these energy-independent analyses, we used separate $^1S_0$ phases for the (p,p) and (n,p) data, in accordance with our handling of the energy-dependent analyses. As can be seen, the uncertainties in the $^1S_0$ phase obtained from fitting just to (n,p) data are very large. At 330 and 425 MeV, it was necessary to remove the splitting in the $^1S_0$ phase in order to keep from having large uncertainties in the $I=0$ phases.

Comparison of Table VIII in the present paper with Tables IV and XV of Paper IX shows that the energy-independent solutions are very similar to one another[20] at energies of 210 MeV and below. However, at 330 and 425 MeV, the new energy-independent solutions are somewhat different from the older ones with respect to the $I=0$ phases. In particular, the new solution at 425 MeV has $I=0$ phases that closely resemble those of the eight-parameter solution of Table XV in Paper IX. When we added the new Chicago-Wisconsin data,[4] the 425-MeV solution went into a form in which the triplet-G phases closely resemble their values as calculated theoretically from OPE.

In Paper IX, we listed error matrices and second-derivative matrices for the energy-independent solutions. The corresponding matrices from the present paper are very similar to the published matrices, especially for energies at 210 MeV and below. We will not publish the updated matrices corresponding to the solutions in Table VIII, but they can be obtained by writing to the authors.

Comparison of the phases in Table VIII with those in Tables IV, VI, and VII shows that whereas the $I=1$ phases are everywhere in good agreement, the $I=0$ phases show considerable scatter. At energies of 142, 210, and 425 MeV, where (n,p) triple-scattering data are available (see Table III), the $I=0$ single-energy phases are reasonably well defined and in agreement with the energy-dependent results. However, at energies below 142 MeV, and also at 330 MeV, the only available (n,p) data are differential cross-section, total cross-section, and polarization measurements (and four C_{NN} data at 23.1 MeV). These data are not sufficient to permit an unambiguous determination of the $I=0$ phases. Thus, while the single-energy $I=0$ solutions at 25, 50, 95, and 330 MeV do give excellent fits to the data, they should not be regarded as definitive solutions. In particular, the quoted error limits on these phases

[20] M. D. Miller, P. S. Signell, and N. R. Yoder [Phys. Rev. 176, 1724 (1968)] have completed a recent analysis of the data at 210 MeV, using both split and unsplit $^1S_0$ phases, and they obtained phase-shift values very similar to ours.

are often not realistic, since the phase-shift χ^2 hypersurface at the location of the solution is not parabolic owing to the incompleteness of the data selection.

The single-energy (n,p) solution that we quote here at 330 MeV is considerably different from the one quoted in Paper IX. This difference is due mainly to the improved energy derivatives at 330 MeV that we obtained from the present energy-dependent analysis. This improvement is principally because of the addition of new triple-scattering data at 425 MeV. To see the effect of this difference on the predicted observables, we made a comparison of the predictions from the two solutions. This showed that the R, C_{NN}, and C_{KP} observables are quite different in the two cases. The newer solution in the present paper has observable predictions that are in reasonable agreement with those of the energy-dependent analysis at 330 MeV.

VII. CONCLUSIONS

The (p,p) data are now complete enough and accurate enough that phase shifts can be determined with precision over the energy span from threshold to 450 MeV. The energy-dependent solution, which goes properly into the effective-range expansion at low energies, gives a good fit to the low-energy (p,p) data when all of the necessary vacuum-polarization corrections are applied. Energy-dependent and energy-independent solutions are in good agreement, which indicates that form limiting is not a factor. Since a precise fit ($M=1.05$) to 1076 (p,p) data in the 1–450-MeV energy span required only 26 free parameters to represent 14 free phases, the phenomenological forms chosen to represent the energy dependences of the phase shifts are useful ones. The interpolative and predictive powers of the (p,p) energy-dependent solution at all energies below 450 MeV should, in our opinion, be taken seriously.

The (n,p) data include triple-scattering measurements only near 142, 210, and 425 MeV. At the other energies, the incompleteness in the (n,p) data selection leads to ambiguous results for the $I=0$ phases. At these three energies, the $I=0$ phases are reasonably well defined, although possible systematic errors due to the use of deuterium targets for most of the triple-scattering measurements are hard to evaluate. The single-energy results at 25, 50, 95, and 330 MeV for the $I=0$ phases should be used with some caution. Although they give excellent fits to the data, they are not definitive solutions. This is an argument for going to an energy-dependent analysis. However, the inherent uncertainties in the $I=0$ scattering matrix do carry over to some extent into the energy-dependent analysis, and we in fact give two versions for the energy-dependent $I=0$ solution. The first, given in Table VI, is what we obtain from the data directly. The second, given in Table VII, is what we obtain by matching the Wisconsin (n,p) $\sigma(\theta)$ shape at 24 MeV exactly, and thereby forcing the ϵ_1 phase shift to remain positive at low energies, in accord with theoretical expectations. Both solutions give very good fits to the 990 (n,p) data, with M values of 1.11 and 1.15, respectively.

By splitting the $^1S_0$ phase into (p,p) and (n,p) components, and letting each approach its proper effective-range limit at low energies, we obtain precision fits to the (n,p) data down to at least 0.5 MeV. Thus the data are now precise enough at low energies to clearly reveal charge-dependent effects. As Fig. 2 shows, the (p,p) and (n,p) $^1S_0$ phases attain nearly the same values in the energy region 100–200 MeV. The splitting that occurs at the higher energies is probably anomalous[8] and may be due in part to lack of a reliable differential cross-section measurement at 425 MeV. Charge-dependent effects in other phases are not yet indicated by analysis of the existing data.

Experimentally, the greatest need is for precision (n,p) scattering measurements around 330 MeV and below 100 MeV. In particular, (n,p) differential-cross-section measurements are needed below 60 MeV. Theoretically, potential modelists should now be able to extract more information from the nucleon-nucleon data (or, equivalently, from the phase-shift second-derivative matrices) than was obtained from earlier models fitted to a more incomplete and more inaccurate data selection.

ACKNOWLEDGMENTS

We would like to thank R. J. Slobodrian, H. E. Conzett, J. C. Davis, D. Measday, H. H. Barschall, N. Booth, J. Hopkins, O. N. Jarvis, B. Rose, and P. Catillon for helpful discussions about the data. Special thanks are due to S. C. Wright for supplying us with data the same day they were measured. Theoretical discussions by one of us (M. H. M.) with J. Perring, Yu. Kazarinov, F. Lehar, P. Signell, Z. Janout, A. Pazman, L. Lapidus, J. Bystricki, V. I. Lendyell, and Ya. Smorodinsky are gratefully acknowledged. Finally, we thank R. A. Bryan for his help in some of the early work in this program, and S. Fernbach and E. Teller for their support of this research.